# FEM Evaluation of Asymmetrical Four-Point Bending Test of SiC/SiC Composite Joints †

Hisashi SERIZAWA*, Charles A. Lewinsohn** and Hidekazu MURAKAWA***

Abstract

*Reliable methods for joining ceramics, for use at elevated temperatures, are enabling technologies for the successful utilization of ceramic components. In this study, the stress distribution of a SiC/SiC composite specimen containing a butt joint consisting of reaction-formed silicon carbide tested by the asymmetrical four-point bending test was precisely analyzed by the finite element method as a means of evaluating the applicability of analytical results. In the case without the effect of the thermal residual stresses, the shear stress distribution at the interface between the base and the joint almost agreed with the analytical theory. For the case with the residual stress, however, the shear stress near the surface was very large and the possibility of an initial crack induced by the residual stress was considered. Moreover, a study of the effect of joint thickness on the residual shear stress indicated that the thickness should be greater than 100 μm to prevent specimen deformation.*

KEY WORDS: (SiC/SiC Composite) (Ceramics) (Joint) (Finite Element Method) (Residual Stress) (Shear Strength) (Asymmetrical Four-Point Bending Test)

## 1. Introduction

Ceramic composites are promising candidate materials for high heat flux components. Silicon carbide based fiber reinforced silicon carbide composites (SiC/SiC composites) are one of the most attractive materials for high temperature applications because of their high temperature properties, chemical stability and good oxidation and corrosion resistance[1-4]. For fabricating large or complex shaped parts of SiC/SiC composites, the technique of joining between simple geometrical shapes is considered to be an economical and useful method. Joints must retain their structural integrity at high temperatures and must have mechanical strength and environmental stability comparable to the bulk materials.

As a result of R & D efforts, various types of joining between ceramic composites have been provided; for example, mechanical fastening, adhesive bonding, welding, brazing and soldering[5-8]. Most of these techniques, however, suffer from various limitations such as the requirement of high temperature processing or hot pressing, a large mismatch of thermal expansion coefficient between the joint material and the base materials, a lower temperature limit than the bulk materials, and so on. Recently, an affordable, robust ceramic joining technology (ARCJoinT$^{TM}$) has been developed as one method to solve the above problems[8].

To establish useful design databases, the mechanical properties of joints must be accurately measured and quantitatively characterized. There are many types of experimental techniques for measuring the mechanical strength of joints at high temperatures: (1) tensile or bending tests to measure the tensile strength of joints, (2) single- & double-lap joint tests, (3) double-notch shear in compression tests, or (4) asymmetrical four-point bending tests to measure the shear strength[8-10]. Among these methods, the asymmetrical bending test seems to be most economical due to the requirement of small test specimens with simple geometry[10]. The shear stress of this test has been evaluated according to the analytical method for homogeneous materials, although the stress state of a joint specimen is different from that of a uniform one. Moreover, there are likely to be thermal residual stresses in joints because of the fabrication process and the mismatch of thermal expansion coefficients. Therefore, in this paper, the stress distribution under the asymmetrical four-point bending

† Received on May 31, 2001
* Research Associate
** Pacific Northwest National Laboratory
*** Professor

Transactions of JWRI is published by Joining and Welding Research Institute of Osaka University, Ibaraki, Osaka 567-0047, Japan.

test was precisely examined by using the finite element method and the effects of the residual stress and the joint thickness were studied.

## 2. FEM Model

**Figure 1** shows a schematic illustration of the asymmetrical four-point bending test, where the butt joint is in the middle of specimen. According to conventional elasticity theory for homogeneous materials[10], the maximum shear stress, $\tau_{max}$, occurs at the center of the specimen, namely the midpoint of the joint, and has a value is,

$$\tau_{max} = \frac{3P(L_1 - L_2)}{2BW(L_1 + L_2)} \quad (1)$$

where $P$, $B$ and $W$ are the applied load, specimen thickness and specimen width, respectively. As shown in Fig. 1, $L_1$ and $L_2$ are the outer and inner span lengths, and according to the theoretical analysis the ratio $L_1/L_2$ should be more than 2 to induce shear failure at the joint. Ünal *et al.* reported that this asymmetrical test for a $30^L$ x $3.2^W$ x $4^B$ mm$^3$ specimen provided accurate results with $L_1$ = 28 mm and $L_2$ = 6 mm [10]. In this study, $L_1$ and $L_2$ were chosen to be 44 and 12 mm, respectively, for a $50^L$ x $3^W$ x $4^B$ mm$^3$ specimen. These values were selected to support our ongoing experimental research, which will be reported in the future. The diameter of the pins was chosen to be 4.75 mm.

SiC/SiC composites jointed by reaction-formed silicon carbide, via the ARCJoinT$^{TM}$ method[8], in which the thickness of the joint, $t$, was set to 50 μm, were selected as the joint material for this study. The relevant material properties are shown in **Table 1** [11-14]. Although the mechanical properties of SiC/SiC composites should be anisotropic, the properties were assumed to be isotropic since the difference between the properties of the composite and the joint material is significantly larger than those due to the composite anisotropy. Furthermore, the shear stress at the interface of the composite and the joint is the focus of this analysis. Due to the brittleness of the ceramic materials, the FEM calculations were conducted assuming linear elastic behavior in two dimensional plain strain using commercial FEM programs: MSC.Marc 2000 for the FEM code and MSC.Mentat 2000 for the pre-post program. he total number of elements and nodes for the joint material were 13600 and 13923, respectively, and the element sizes were decided by continuously refining the mesh until approximate convergence with the numerical solution was achieved.

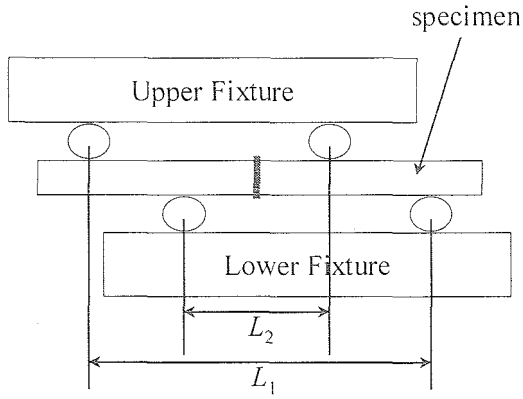


**Fig.1** Schematic illustration of asymmetrical four-point bending test.

## 3. Effect of FEM Model Type

To analyze the asymmetrical bending test, three types of FEM models were used in this study. **Figure 2** shows the schematic illustrations of these models. The first model represented the asymmetrical test as precisely as possible, where the four pins were deformable and the contact points between the pins and the specimen could move, so this model was denoted as a "Deformable Pin Model". In the second model the pins were assumed to be rigid though the contact points were movable, therefore this model was denoted as a "Rigid Pin Model".

**Table 1** Materials properties used in FEM analysis[11-14].

| | SiC/SiC | RB-SiC (Joint) | Monolithic SiC (Pin for Load) |
|---|---|---|---|
| Young's Modulus (GPa) | 300 | 393 | 408 |
| Poisson's Ratio | 0.3 | 0.19 | 0.14 |
| Density (Mg/m$^3$) | 2.50 | 2.90 | 3.00 |
| CTE ($10^{-6}$/K) | 3.0 | 4.3 | |

**Table 2** Boundary conditions of three types of FEM models.

| | |
|---|---|
| Deformable Pin Model | |
| 1 | x-direction = 0 at $C_1$ (x = 0, y = $W$/2) |
| 2 | x-direction = 0 at $C_3$, $C_4$, $C_5$, $C_6$ (Center of Pins) |
| 3 | x-direction = 0 at $P_5$, $P_6$, $P_7$,$P_8$ (Contact Points between Pins and Rigid Surfaces) |
| 4 | y-direction = 0 at $P_7$, $P_8$ |
| 5 | Rigid Surface 2 : y-direction = 0 |
| 6 | Rigid Surface 1 : y-direction = -0.05 mm for 1 step (total 2000 steps ) |
| Rigid Pin Model | |
| 1 | x-direction = 0 at $C_1$ (x = 0, y = $W$/2) |
| 2 | Rigid Surface 2 : x-direction = 0, y-direction = 0 |
| 3 | Rigid Surface 1 : x-direction = 0, y-direction = -0.05 mm for 1 step (total 2000 steps ) |
| Point Load Model | |
| 1 | x-direction = 0 at $C_1$ (x = 0, y = $W$/2) |
| 2 | x-direction = 0 at $P_1$, $P_2$, $P_3$,$P_4$ (Contact Points between Specimen and Pins) |
| 3 | y-direction = 0 at $P_3$, $P_4$ |
| 4 | y-direction = -0.05 mm for 1 step at $P_1$, $P_2$ (total 2000 steps) |

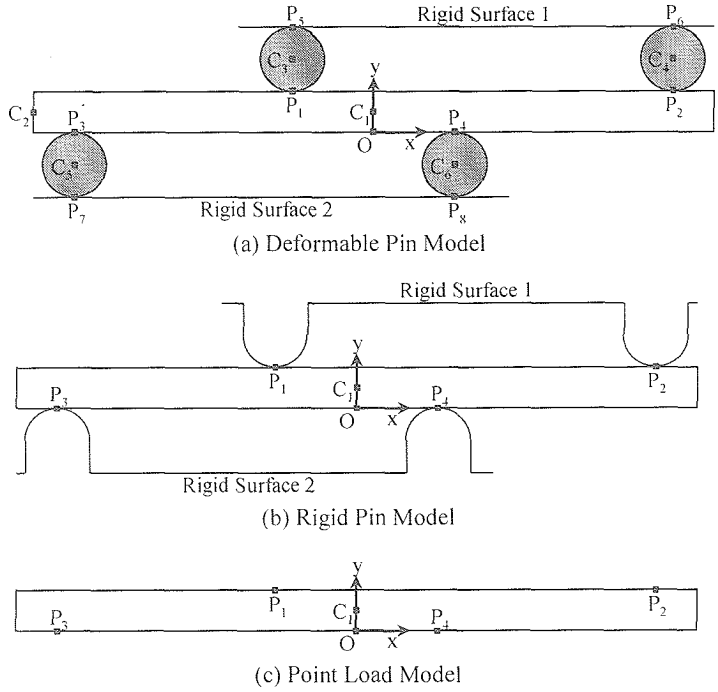


**Fig.2** Schematic illustration of three types of FEM models.

The third one was a classical model for a bending test, where the contact points were set not to move and the loads were applied at these points. The latter model was denoted as a "Point Load Model". The boundary conditions of these models are shown in **Table 2**. For the first two cases, the loads were applied by a constant movement of an upper rigid surface along the y-axis direction. In the last model, the upper two contact points ($P_1$ and $P_2$) moved along the direction of the y-axis, causing load to be applied to the specimen.

The load-displacement curves predicted by the three FEM models are shown in **Fig.3(a)**, and the relationship between the computed shear stress at the center of the specimen and the displacement are also shown in **Fig.3(b)**. In both figures, the differences between the Deformable Pin Model and Rigid Pin Model were relatively small and were considered to be due to the deformation of four pins. On the other hand, the load and the shear stress predicted by the Point Load Model were much larger than the other two models for the same displacement. The calculated shear stress and the shear stress according to Eq.(1) were compared. For the Deformable Pin Model and the Rigid Pin Model, the agreement with the theoretical analysis was very good. On the other hand, the shear stresses predicted by the Point Load Model were significantly different, as shown in **Fig.4**. This disagreement illustrates the importance of using contact points that are free to rotate in experimental measurements, and the difference between stresses on specimens when the contact points are

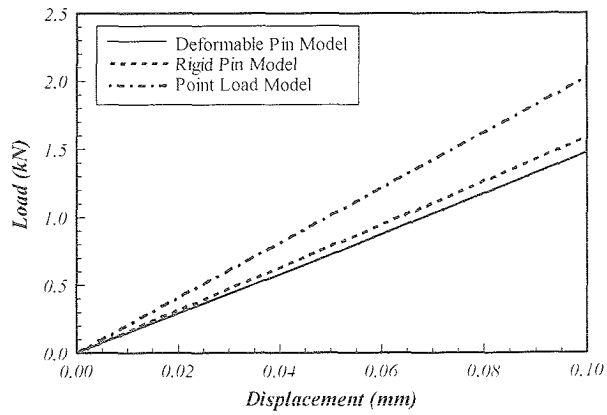


(a) Load-Displacement Curves of Three Types of FEM Models

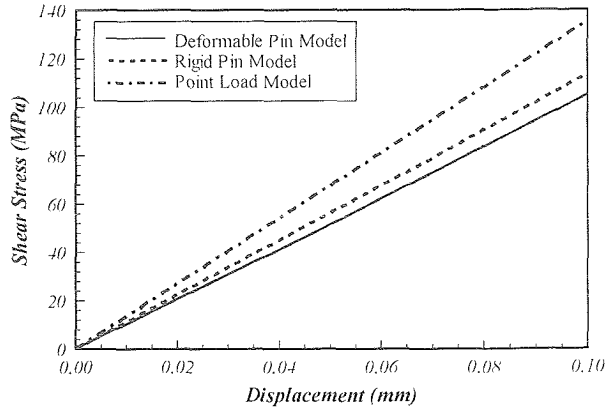


(b) Relationships between Shear Stress at Center of Specimen and Displacement

**Fig.3** Effect of FEM model type on computational load and shear stress.

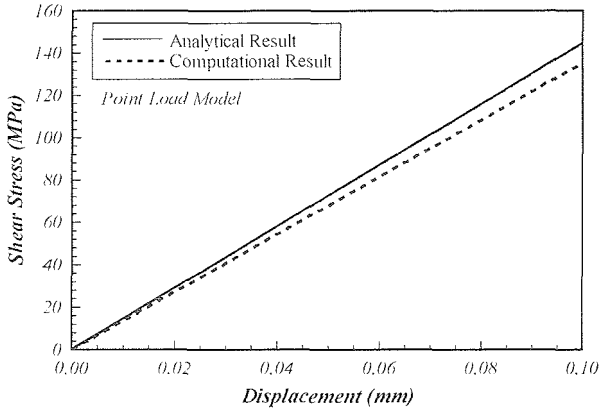


**Fig.4** Difference between analytical shear stress and computational shear stress for Point Load Model.

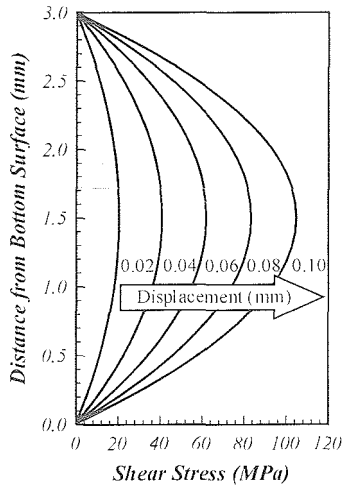


**Fig.5** Shear stress change at the interface between SiC/SiC composite and joint (x = $t$/2).

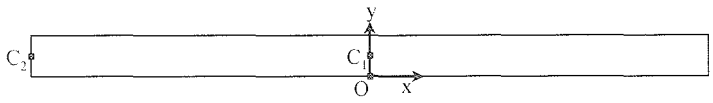


Boundary Conditions

1. Only specimen (No Pins)
2. x-direction = 0 at $C_1$ (x = 0, y = W/2)
3. y-direction = 0 at $C_1$ and $C_2$ (x = -L/2, y = W/2)
4. No stress in specimen at 1250 °C (1325 °C, 1425 °C)
5. Room temperature : 25 °C
6. Only thermal expansion

**Fig.6** Schematic illustration and boundary conditions for the calculation of thermal residual stress.

constrained or free to move. Assuming that the motion of contact points is unconstrained during experiments the Deformable Pin Model appears the most suitable FEM model to compare with experimental results. Therefore this model was used in the following calculations.

## 4. Effect of Joint

To examine the effect of joint materials on the shear stress using the Deformable Pin Model, the predicted shear stress at the center of specimen (x = 0, y = $B$/2) was compared with the predicted shear stress at the middle of the interface between SiC/SiC composite and the joint (x = -$t$/2 or $t$/2, y = $B$/2). According to the calculated results, the difference between these predicted shear stresses was very small and only 0.01 % at 100 μm displacement of the specimen. The reason for such a small difference was considered to be the small difference between the elastic properties of the SiC/SiC composite and the joint. **Figure 5** shows the predicted shear stress change at the interface (x = $t$/2). In accordance with elasticity theory, the maximum stress was predicted at the middle of specimen in the specimen width (y = $B$/2).

## 5. Effect of Thermal Residual Stress

For the ceramic composite materials, it was reported that the effect of thermal residual stress on the mechanical properties was large because the maximum temperature in the fabrication process is more than 1000 °C[15-17]. Although, in the case of ARCJoinT™, the difference in thermal expansion coefficient between the joint and base materials is relatively small, the effect of residual stresses on the shear stresses due to the asymmetrical bending test is unknown. This effect was studied by using the Deformable Pin Model.

**Figure 6** shows the schematic illustration and boundary conditions for the calculation of thermal residual stress. In some previous reports, the boundary conditions used for calculating the thermal residual stresses varied[15,16]. There are, however, only three necessary conditions for each specimen in the two dimensional FEM analysis that prevent movement of the specimen, namely translation and the rotation. The maximum temperature in the fabrication process of ARCJoinT™ is between 1250 and 1425 °C[8,17]. Therefore the effect of the residual stresses was examined for three cases, in which the maximum temperatures were 1250, 1325 and 1425 °C. The residual

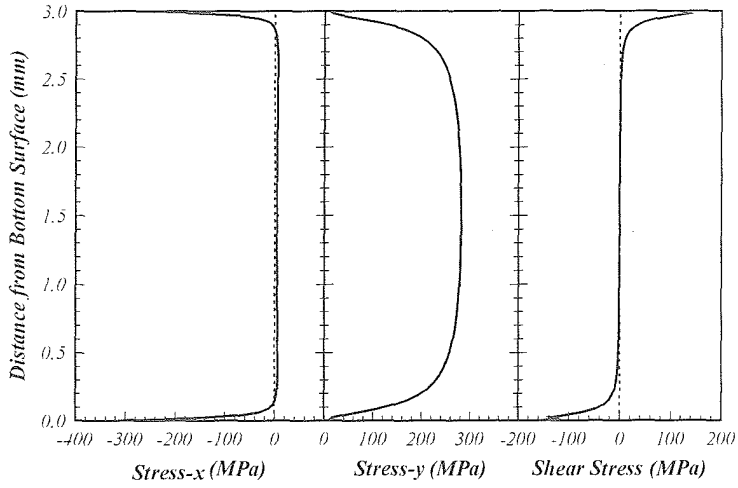


Fig.7 Thermal residual stress distributions at the interface (x = $t$/2) for the case of 1250 °C maximum temperature.

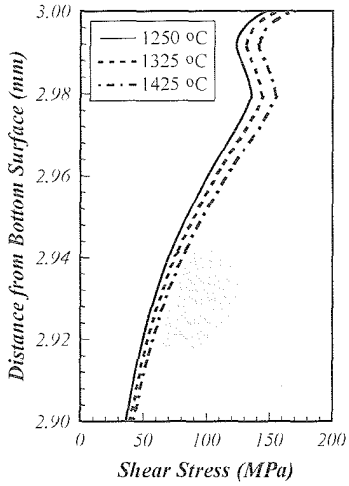


Fig.8 Effect of maximum temperature on residual shear stress on the interface.

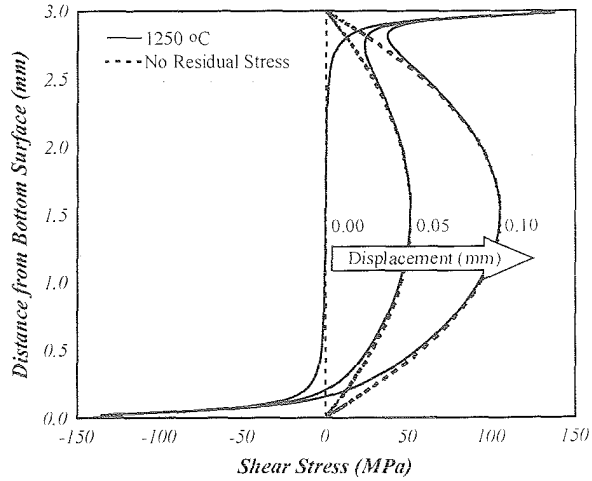


Fig.9 Shear stress changes with and without the residual stress on the interface.

stress was calculated assuming a constant temperature decrease from the maximum temperature to room temperature (25 °C), where the elastic and thermal properties (shown in Table 1) were assumed to be independent of the temperature change.

The calculated thermal residual stress distributions at the interface (x = $t$/2) for the case of 1250 °C are shown in **Fig.7**. As expected, the predicted axial stresses (stress-x and stress-y) were line symmetrical about the mid-plane of the width (y = $B$/2) and the predicted shear stress was point symmetrical about the center of interface (x = $t$/2, y = $B$/2). For the stress-x and the shear stress, there were large residual stresses on the specimen surface. On the other hand, the predicted residual stress of stress-y on the surface was small. The effect of the maximum temperature on the calculated residual axial stresses (stress-x and stress-y) was found to be small, so only the change of predicted shear stress near the upper surface is shown in **Fig.8**. From this figure, the calculated residual shear stress was found to increase slightly with increasing maximum temperature. Therefore, only the case of 1250 °C maximum temperature will be discussed further.

Out of all the predicted stresses, only the calculated shear stress changed significantly, due to thermal residual stresses, under the asymmetrical test. The calculated shear stress with and without the residual stress at the interface is shown in **Fig.9**. Although the calculated shear stress distributions on the specimen surfaces were very different between these two cases, the calculated shear stresses at the middle of specimen width were almost the same at any displacement. Therefore, the calculated shear stress near the upper surface differed from that without residual stresses, and the predicted shear stress increased slightly with the increment of displacement as shown in **Fig.10**. From these figures, it was found that the effect of residual stresses on the shear strength between SiC/SiC composite and reaction-formed joint material would be insignificant if the shear strength of the material is larger than the residual shear

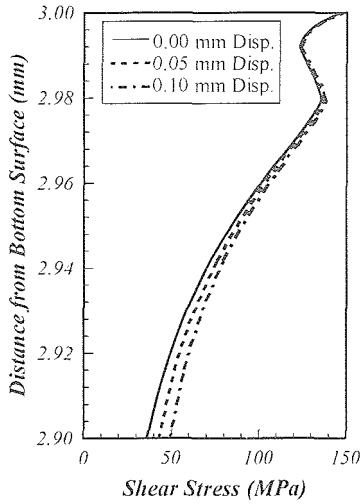


**Fig.10** Shear stress change with the residual stress on the interface.

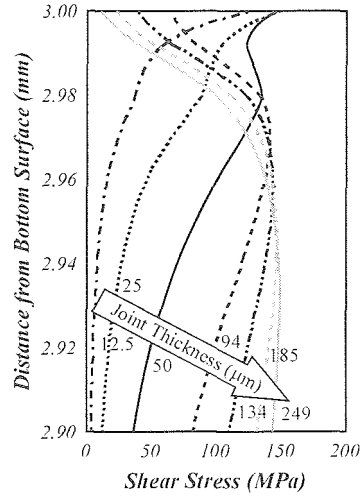


**Fig.11** Effect of joint thickness on residual shear stress at the interface.

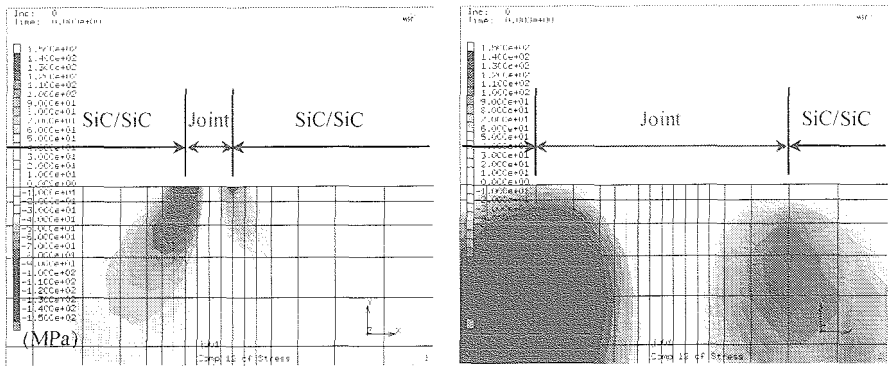


(a) 25 μm Joint Thickness (b) 134 μm Joint Thickness

**Fig.12** Shear stress distributions on near the surface for the cases of 25 and 134 μm joint.

stress near specimen surfaces. The four-point flexural strength for the ARCJoinT$^{TM}$ specimen of SiC/SiC composites was reported to be about 65 MPa[8], and the shear strength is likely to be smaller than the flexural strength. Although the calculated residual stresses might not be exactly correct, since the temperature dependency of elastic and thermal properties were ignored, the true residual stress should be close to the calculated value. Therefore, for this joint material, it was concluded that specimens might contain initial cracks near the surface and that fracture is likely to initiate from these cracks.

## 6. Effect of Thickness of Joint

Due to the structural design and the fabrication process, the thickness of the joint generally varies, so the effect of the joint thickness on the thermal residual stress was examined. In this research, the original mesh division was not changed in order to remove the effect of the mesh division on the stress distributions. The effect of the joint thickness was studied for the cases of 12.5, 25, 50, 94, 134, 185 and 249 μm joints, where the calculation results of the 12.5 μm joint were relatively

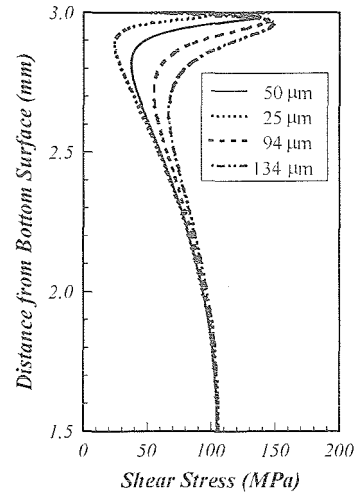


**Fig.13** Effect of joint thickness on shear stress at the interface under 100 μm displacement.

uncertain since this joint was divided into only two FEM elements along the joint thickness direction.

**Figure 11** shows the effect of the joint thickness on the residual shear stress at the interface. From this figure, the calculated shear stress on the surface was found to

decrease with increasing joint thickness, the point of the maximum predicted shear stress gradually moved from the surface into the inside, and the maximum value of the calculated shear stress increased very slightly with increasing joint thickness. The predicted shear stress distributions near the surface for the cases of 25 and 134 μm joints are shown in **Fig.12**. It can be seen clearly that the point of the largest residual stress moves to the inside of the specimen along the interface with increasing thickness of the joint. Therefore it is possible that there might be an initial crack not at the surface but in the inside of the specimen for the joints that are over 100 μm thick. Moreover, the thickness of the joint should be more than 100 μm to keep the shape of the specimen. On the other hand, the shear stress at the middle of the specimen width on the interface ($x = t/2$, $y = B/2$) under 100 μm displacement was almost independent of the joint thickness as shown in **Fig.13**.

From the above discussions, regardless of the joint thickness, the asymmetrical four-point bending test was considered to be useful for obtaining the shear strength according to the analytical theory for the case with no initial crack induced by residual shear stress. Since it is likely that there are initial cracks in many cases, the crack propagation process under the asymmetrical bending test must be analyzed precisely in the future.

## 7. Conclusions

To examine the accuracy of the analytical theory for the asymmetrical four-point bending test of the joint material between SiC/SiC composite and ARCJoinT™, the stress distribution under this test was precisely analyzed by using the finite element method. Furthermore, the effect of the residual stress and the joint thickness was also studied. The conclusions are as follows,

(1) In order to analyze contact problems such as the asymmetrical bending test, the constraints on motion of the contact points have a large effect on the stress distribution and have to be taken into account for comparison with experimental results.

(2) In the case without the effect of the thermal residual stresses, the calculated shear stress distribution at the interface between the base and the joint almost agreed with the analytical theory.

(3) Although the residual stress did not affect the predicted shear stresses at the mid-plane of specimen width under the asymmetrical bending test, the calculated residual shear stress near the surface was very large and the possibility of an initial crack induced by the residual stress was considered. The effect of maximum temperature during the fabrication process on the residual stresses, however, was found to be small.

(4) The effect of the joint thickness on the shear stress at the middle of specimen width on the interface was found to be small, but the residual stress distribution near the surface was significantly affected and it is thought that the thickness of a joint should be over 100 μm to prevent specimen deformation.

## Acknowledgements

The authors are extremely grateful to Dr. M. Singh, NASA Glenn Research Center, for stimulating discussions and valuable information. The work was supported by Core Research for Evolutional Science and Technology : Advanced Material Systems for Conversion of Energy. This work was also supported by The Office of Fusion Energy Science under U.S. Department of Energy (DOE) contract DE-AC06-76RLO 1830 with Pacific Northwest National Laboratory, which is operated for DOE by Battelle.

## References

1) J. R. Strife, J. J. Brennan and K. M. Prewo, Ceram. Eng. Sci. Proc., 11 [7-8], 871 (1990).
2) R. H. Jones and C. H. Henager, Jr., J. Nucl. Mater., 212-215, 830 (1994).
3) R. H. Jones, C. A. Lewinsohn, G. E. Youngblood and A. Kohyama, Key Engineering Materials, 164-165, 405 (1999).
4) H. Serizawa, C. A. Lewinsohn, G. E. Youngblood, R. H. Jones, D. E. Johnston and A. Kohyama, Ceram. Eng. Sci. Proc., 20 [4], 443 (1999).
5) C. R. Bates, M. R. Foley, G. A. Rossi, G. J. Sandberg and F. J. Wu, Ceramic Bulletin, 69, 3, 350 (1990).
6) J. D. Cawley, Ceramic Bulletin, 68, 9, 1619 (1989).
7) R. Larker, A. Nissen, L. Pejryd and B. Loberg, Acta Metall. Mater., 40, 11, 3129 (1992).
8) M. Singh, Key Engineering Materials, 164-165, 415 (1999).
9) Y. Ishiguro, T. Akatsu, Y. Tanabe and E. Yasuda, Key Engineering Materials, 164-165, 171 (1999).
10) Ö. Ünal, I. E. Anderson and S. I. Maghsoodi, J. Am. Ceram. Soc., 80 [5], 1281 (1997).
11) K. D. McHenry and R. E Tressler, J. Am. Ceram. Soc., 63 [3-4], 152 (1980).
12) "Materials Properties Standard 2000", Coors Ceramics Company, Golden, Colorado (1999).
13) "Physical Properties of Hexoloy® SA Silicon Carbide", Carborundum Corporation, Niagara Falls, NY (2000).
14) K. Kageyama and I. Kimpara, Key Engineering Materials, 164-165, 127 (1999).
15) L. J. Ghosn, J. I. Eldridge and P. Kantzos, Acta Metall. Mater., 42, 11, 3895 (1994).
16) K. Honda and Y. Kagawa, Acta Metall. Mater., 43, 4, 1477 (1995).
17) C. A. Lewinsohn, R. H. Jones, M. Singh, T. Shibayama, T. Hinoki, M. Ando and A. Kohyama, Ceram. Eng. Sci. Proc., 20 [3], 119 (1999).